JOURNAL OF APPLIED PHYSICS VOLUME 92, NUMBER 6 15 SEPTEMBER 2002

Effects of surface treatments on the adhesion of Cu and Cr/Cu metallizations to a multifunctional photoresist

J. Ge and J. K. Kivilahti
Laboratory of Electronics Production Technology, Helsinki University of Technology, P.O. Box 3000, Helsinki FIN-02150 HUT, Finland

(Received 13 November 2001; accepted for publication 29 May 2002)

The effects of chemical, plasma, and reactive ion etching (RIE) treatments on the adhesion of Cu and Cr/Cu to the multifunctional polymer were investigated. The adhesion was measured with the newly developed pull test. The polymer surfaces were characterized by the x-ray photoelectron spectroscopy, atomic force microscopy, and surface free energy measurement. The failure modes were examined with the scanning electron microscopy and energy-dispersive spectroscopy. It was found that the adhesion of Cu and Cr/Cu to the highly functional photoresist was poor, regardless of the chemical, plasma, and reactive ion etching treatment with either O_2 or CF_4 used. However, the RIE pretreatment with the gas mixture (O_2+CF_4) of the photoresist surface increased the adhesion of sputtered Cr/Cu to the photoresist remarkably, and the failure mode was cohesive within the photoresist. Furthermore, the RIE pretreatment with pure oxygen gave rise to the needle-like surface together with virtually no introduced reactive functional groups, whereas the RIE with O_2-rich gas mixture of O_2+CF_4 resulted in the relative smooth polymer surfaces and the newly formed C=O/O–C–O and O–C=O functionalities were incorporated on the treated surface with the increased polar surface free energy. The adhesion mechanism based on the experimental adhesion results and the surface characterizations of the polymer is proposed and discussed. © *2002 American Institute of Physics.* [DOI: 10.1063/1.1495528]

I. INTRODUCTION

The technological basis of future portable electronics is established on high performance integrated circuits which are densely connected to passive components in low cost and highly functional buildup modules but, while striving for ever higher performance and functionality more fundamental requirements are encountered in packaging and in printed wiring board fabrication. Even though novel packaging solutions and high density microvia boards have been developed recently, broader bandwidths and especially higher frequencies of future low-cost wireless communication devices demand more disruptive solutions. One such a solution is to integrate silicon chips and passive components inside high density buildup substrates.[1] This can be carried out either with fully additive or semiadditive techniques utilizing photodefinable polymers and chemical metal deposition processes.[2] It is emphasized, however, that the great technical advantages provided by these highly integrated buildup modules depends primarily on good adhesion between thin polymer and metal layers.

Adhesion between dissimilar materials depends on the chemical, physical, and morphological nature of the interface. Because of the surface inertness of polymers, the adhesion of metal to polymer is generally weak. The highly functional photoresist (SU-8), which has been introduced recently to microelectromechanical systems (MEMS) applications, has an advantage of good processability and high resolution. Therefore, the material is also exceptionally attractive for the integration of active and passive components inside high-density multilayer printed wiring boards; the technology which is gaining increasing importance in manufacturing most advanced consumer electronics. However, it is extremely difficult to obtain sufficient adhesion of Cu to this photoresist because of its high crosslinking nature. Even though this drawback has attracted much attention, and many techniques have been developed to improve the adhesion of metal to polymers such as chemical treatment, plasma, and ion beam surface modification,[3–7] no study has been carried out on the improvement of the adhesion between Cu and the photoresist. Metallization of a polymer is typically performed by first etching the polymer surface to increase roughness, which is then followed by electroless deposition of copper. Strong adhesion has been achieved by mechanically anchoring copper into the fine cavities of roughened polymer surface.[8] However, all the available photopolymers cannot be easily microroughened, and there is an increasing number of applications, where roughened polymer surfaces have deleterious effects on the performance of electronics, especially in high frequency broadband wireless communication.[9,10] Accordingly, sufficient adhesion of metals to smooth polymer surfaces must be achieved. The alternative metallization method is the use of sputter-deposited metal as a seed layer. Adhesion-promoting metals such as Cr, Ti, or W are often used as the interlayer to enhance the adhesion. Some studies have reported that Cr is the most effective adhesion promoter metal.[11,12] Therefore, chromium is used between copper and the photoresist in this study. It is noted that in sputtering technique, the adhesion of sputter-deposited metal to modified surface occurs primarily through chemical bonding.

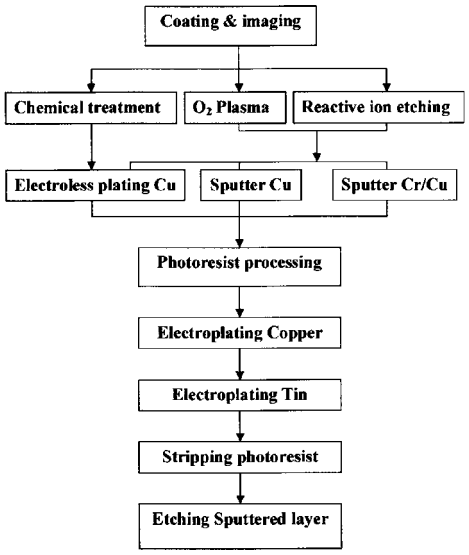

FIG. 1. Flow chart of fabrication process of the test pads for the adhesion measurement.

In the present work the effects of chemical, plasma, and RIE treatment on the adhesion of Cu and Cr/Cu to the multifunctional photoresist will be investigated. The adhesion will be measured with the newly developed pull test. The failure modes will be examined with the optical microscopy, scanning electron microscopy (SEM), and energy-dispersive spectroscopy (EDS). The polymer surfaces are characterized by the x-ray photoelectron spectroscopy (XPS), atomic force microscopy (AFM), and surface energy measurements to correlate the adhesion mechanism to the pull strength values.

II. EXPERIMENT

A. Preparation of specimens

The flow chart of the fabrication process of the test pads is shown in Fig. 1. Epoxy with E-glass reinforcement (FR4 from NELCO) was used as the substrate. The photosensitive epoxy solution (SU-8 from MicroChem Corp.) was spin coated onto the substrate to a thickness of ~15 μm. SU-8 is a negative, epoxy-based resist which has multifunctional epoxy side groups proving a very dense three-dimensional network of crosslinking when cured. After spin coating, the board was soft baked, ultraviolet (UV)-exposed (15.5 mW/cm^2) and cured.

Three types of surface treatments were carried out. The first was the chemical treatment, which consists of three water-based steps: swelling, etching and reduction, and then followed by the activation and electroless deposition. The details are reported in a previous article.[8] In the second treatment the specimens were processed in pure oxygen plasma at rf power 80 W for 5–20 min. The third method was reactive ion etching (RIE) with pure O_2, pure CF_4, and the mixture of O_2+CF_4. The results shown below are from RIE treatment unless otherwise stated. In the reactive ion etching system, the plasma was produced in the region between two electrodes, and the sample was placed directly below the plasma, on a plate shielding the lower electrode, which was powered by a 13.56 MHz radio-frequency (rf) generator. The surface modification was performed with O_2 and/or CF_4 with flow rates of 5–20 sccm. The rf power varied from 40 to 80 W, and the operating pressure was held in the range between 2.7 and 6.7 Pa. The treatment time ranged from 5 to 30 min. The treated surface was then metallized by electroless plating or sputter deposition. The parameters for the sputter deposition are given in Table I. For one type of samples, only Cu was sputter deposited. For the other type of samples, Cr was deposited, followed by Cu, without breaking the vacuum. Then, a dry film type of photoresist was laminated onto the electroless copper and exposed through a photomask. The trench structure of the resist was formed by developing. Copper was then electrolytically plated on to the resist trench to achieve a thicker copper layer. As an etching resist, a tin layer was plated on the copper surface, and the plating resist was then stripped off. Finally, the copper underlayer was removed with copper etching solution (Ultraincide 35/35 from ALFACHIMICI) and chromium was etched away by a mixed solution of hydrochloric acid and glycerine to form test pads with a diameter of 0.2 cm. Pads for the pull test were then cut from the sample. Copper wire was soldered to the test pads with the eutectic SnPb solder for the pull test.

TABLE I. Deposition parameters.

Parameters	Cr	Cu
Base pressure (Pa)	1.5×10^{-4}	1.5×10^{-4}
Work pressure (Pa)	0.43	0.43
dc power (W)	1000	2000
Ar gas rate (sccm)	50	60
Metal thickness (μm)	0.05	1

B. Adhesion strength measurement

The schematic representation of the adhesion test configuration is given in Fig. 2. A tensile test machine (MTS 858) was used to measure the adhesion strength of Cu and Cr/Cu to SU-8. The diameter of the hole in the center of the test setup was designed to be larger than that of the test pad in order to pull the specimens freely. The specimen was fixed to the test setup, and a copper wire was then clamped in the grip and pulled at a constant ramp rate of 0.001 mm/s. The force required to break the weakest interface was recorded. The test pad area was calculated by assuming that the pad was circular. The adhesion strength was evaluated as the average tensile strength of the twelve specimens prepared under the same conditions.

C. Scanning electron microscopy

The topographies of the treated SU-8 surfaces as well as the fracture surfaces of the metallized polymer were examined by using a field emission SEM (JSM-6330F, JEOL), operated at 1 or 15 kV.

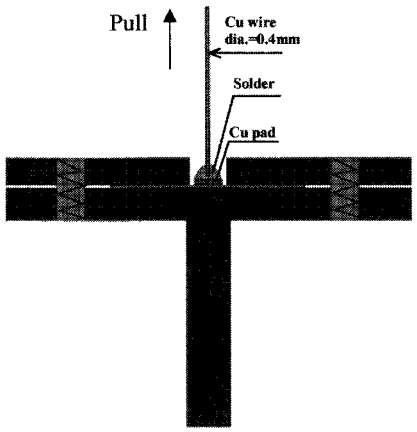

FIG. 2. Schematic representation of the adhesion test configuration.

D. Atomic force microscopy

The surface topography of the untreated and treated photoresist surfaces was characterized on a Nanoscope IIIa atomic force microscope, manufactured by Digital Instrument D3100 Inc. In each case, an area of 5×5 μm was scanned using silicon tips in the tapping mode. The surface roughness of the samples was evaluated in terms of the arithmetic mean of the surface roughness (R_a) and the root mean square of the surface roughness (rms).

E. Surface free energy measurement

The contact angles of water and diiodomethane on the photoresist surfaces were measured by the sessile drop method with Advanced Surface Technology Inc. coniometer equipped with VCA 2500XE video contact angle system. For each sample, the contact angle value is the mean of eight measurements recorded on the different sample surface locations with an experimental error of 2°–3°. From the measured contact angle, the surface free energy (γ_s) was calculated using the classical geometric mean equation:

$$\gamma_L(1+\cos\theta)=2(\gamma_L^d\cdot\gamma_S^d)^{1/2}+2(\gamma_L^p\cdot\gamma_S^p)^{1/2}, \quad (1)$$

where the contact angle (θ) was measured by the liquid drop (volume=0.1 μL) method. γ_S is the sum of the surface free energy contributed from the dispersion (γ_S^d) and polar component (γ_S^p). The dispersive (d) and polar (p) component of the surface free energy of the different liquids (γ_L) adopted in this experiment are $\gamma_L=72.8$, $\gamma_L^d=21.8$, and $\gamma_L^p=51.0$ mJ/m^2 for distilled water, and $\gamma_L=50.8$, $\gamma_L^d=49.5$, $\gamma_L^p=1.3$ mJ/m^2 for diiodomethane.[13,14]

F. X-ray photoelectron spectroscopy

X-ray photoelectron spectra of both untreated and treated samples with RIE were recorded by using an XPS (SSX-10). The monochromatic Al $K\alpha$ x-ray source was operated at an anode voltage of 10 kV and a current of 23 mA, the pressure in the analysis chamber was maintained at 4×10^{-7}–1.2×10^{-6} Pa, and the core-level signals were obtained at a photoelectron takeoff angle (with respect to the sample surface) of 42°±2°. All XPS peaks were referenced to C 1s signal at a binding energy of 284.5 eV representing the C–C and C–H bonds in hydrocarbons.

TABLE II. Adhesion of metal to SU-8 by different surface modification method.

Experiments	Tape test	Pull test	Failure interface
Chemical treatment[a]	×	×	Cu and SU-8 interface
O_2 plasma+Cu	×	×	Cu and SU-8 interface
RIE O_2/CF_4+Cu	√	×	Cu and SU-8 interface
Untreated+Cr/Cu	×	×	Cr and SU-8 interface
O_2 plasma+Cr/Cu	√	×	Cr and SU-8 interface
RIE with O_2+Cr/Cu	√	×	Cr and SU-8 interface
RIE with CF_4+Cr/Cu	√	×	WBL/bulk interface
RIE O_2/CF_4+Cr/Cu	√	>6 N/mm^2	Within SU-8

Note: Fail: ×
Pass: √
[a]Metallization is electrolessly deposited copper.

III. RESULTS AND DISCUSSION

A. Effects of surface treatments on the adhesion of Cu or Cr/Cu to SU-8

The results of testing the adhesion of Cu and Cr/Cu metallization to SU-8 using different surface treatments to enhance adhesion are given in Table II. The adhesion strongly depends on the pretreatment method and by the chemical nature of the deposited metal. The pretreatments of the polymer by the chemical, plasma, and reactive ion etching treatment with either O_2 or CF_4 are not sufficient to achieve the acceptable adhesion. However, the highest adhesion strengths being greater than 6 N/mm^2 were achieved in the case of the SU-8/Cr/Cu system by employing the RIE pretreatment with the gas mixture of oxygen and carbon tetrafluoride. The chemical interaction of copper with polymer is known to be weaker than that of chromium.[15,16] Therefore, the adhesion improvement with the help of RIE polymer surface modification and chromium metallization is emphasized in this study.

In the reactive ion etching system, plasma is produced in the region between two electrodes consisting of a great number of excited atomic, molecular, ionic, and free radical species. Comparing to a pure plasma system, in which the etching is mainly due to the neutral radicals, the RIE method provides higher etch rates because of the combination of ion bombardment with plasma chemical etching. The mechanism of formation of functional groups on polymer surfaces by RIE can be interpreted by a two-step model. The first step is the creation of free radicals by surface bombardment, which has to be sufficient to break the bonds of polymer chains or extract atoms such as hydrogen. The second step is the formation of functional groups by the interaction between the new radicals and reactive species in the plasma.

The effects of different parameters used in RIE surface modification on the adhesion between Cr/Cu metallizations and SU-8 are shown in Figs. 3, 4, and 5. The adhesion strengths were measured by the pull adhesion test developed earlier.[8] Adhesion was poor, if either O_2 or CF_4 was used

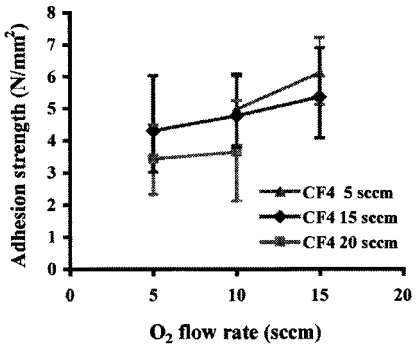

FIG. 3. Adhesion strength of Cr/Cu/SU-8 system as a function of gas flow rate (80 W, 20 min).

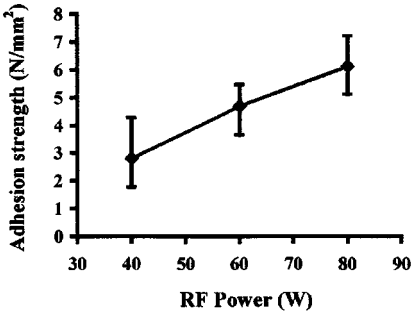

FIG. 5. Adhesion strength of Cr/Cu/SU-8 system as a function of rf power (15 sccm O_2+5 CF_4 sccm,20 min).

(Table II). However, if the gases were mixed properly, the adhesion strength was high with the optimum parameter values. Figure 3 shows the adhesion strengths of the SU-8/Cr/Cu/ system as a function of the gas flow rate at 80 W for 20 min. When CF_4 gas was added to oxygen (15 sccm O_2 +5 sccm CF_4), the pull strength was improved to above 6 N/mm^2. The results show that the RIE treatment with the O_2-rich gas mixture (O_2+CF_4) is an effective method to improve the adhesion of a SU-8/Cr/Cu/multilayer system. It is suggested that the improved adhesion results from the introduction of CF_4 as a coreactant to O_2 because that increases concentrations of oxygen, fluorine, fluorine containing atoms, and radicals.[17,18] This is important since the energetic fluorine and fluorine-containing species are more effective in creating polymer radical sites than the oxygen species. As a result, the generated radical groups by the treatment are capable of capturing oxygen to form functional groups on the treated photoresist surface. Thus, the RIE treatment is well suited to improving the adhesion of the metals to polymers. However, excessive treatment of polymers can result in a weak boundary layer (WBL) that is detrimental to metal/polymer adhesion.[19,20]

The pull strengths of SU-8/Cr/Cu multilayer system as a function of the treatment time are shown in Fig. 4. The treatment was carried out with 15 sccm O_2 and 5 sccm CF_4 at 80 W. The pull strength is improved with increasing treatment time and reaches a maximum at a treatment time of 20 min. However, when the treatment time is increased further, the pull strength is decreased. The low value of adhesion may be attributed to the formation of a WBL as a result of excessive treatment. The effect of the rf power of RIE on the adhesion strength of the SU-8/Cr/Cu system is plotted in Fig. 5. The RIE surface modification at rf power of less than 40 W does not contribute to the adhesion. The pull strength is increased almost linearly from 2.8 N/mm^2 at the rf power of 40 W–6.1 N/mm^2 at 80 W. It is expected that the increasing rf power adds to the amount of radicals, the ion energy flux, and the ion bombardment energy as well as the concentrations of active oxygen and fluorine-containing species at the polymer surface. The adhesion test results show that the optimal RIE condition is with the gas mixture having the flow rate of 15

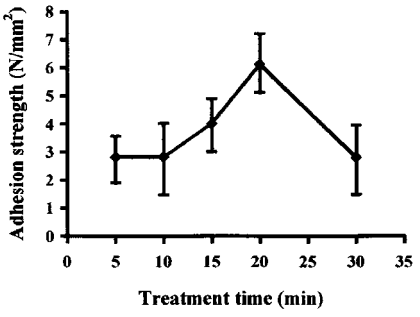

FIG. 4. Adhesion strength of Cr/Cu/SU-8 system as a function of treatment time (15 sccm O_2+5 CF_4 sccm,80 W).

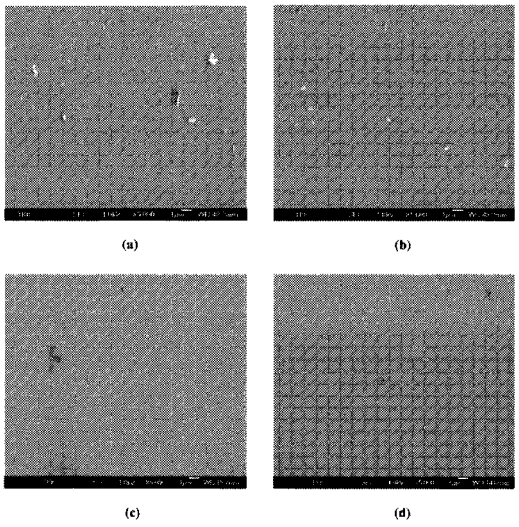

FIG. 6. SEM micrographs of (SU-8 surface) of (a) no treatment; (b) O_2 treatment (15 sccm, 80 W, 20 min); (c) CF_4 treatment (15 sccm, 80 W, 20 min); (d) O_2+CF_4 treatment (15 sccm O_2+5 sccm CF_4,80 W,20 min).

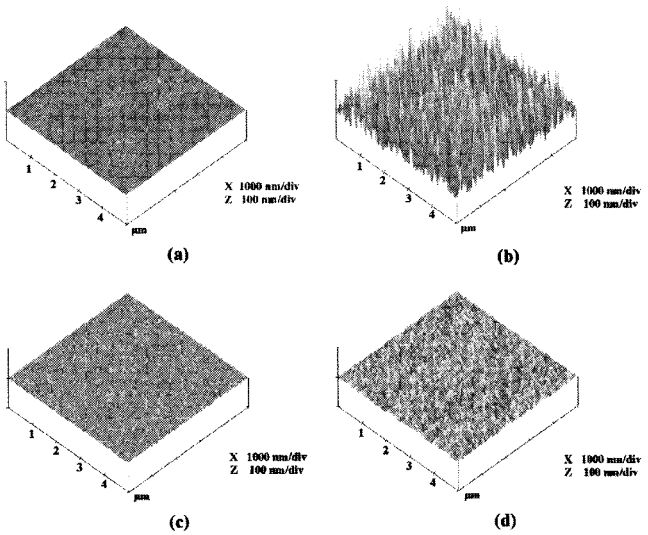

FIG. 7. Atomic force micrographs of SU-8 surface (a) no treatment; (b) O_2 treatment (15 sccm, 80 W, 20 min); (c) CF_4 treatment (15 sccm, 80 W, 20 min); (d) O_2+CF_4 treatment (15 sccm O_2+5 sccm CF_4, 80 W, 20 min).

sccm O_2/5 sccm CF_4 under the pressure of 4 Pa and at the power of 80 W for 20 min.

Generally, the adhesion of metal to polymer is influenced not only by the chemical states of polymer surface but also by the surface topography. To examine the anchoring effect, the polymer surfaces after the RIE pretreatment were investigated with the scanning electron microscopy (Fig. 6). However, no visible changes in the surface topography after the treatment can be detected by SEM.

B. AFM analysis

In order to understand the influence of the pretreatments on the surface topography of the polymer, AFM analyses were performed both for the untreated, and RIE-treated polymer surfaces. The untreated surface is very smooth and featureless as shown in Fig. 7, with a root-mean-square (rms) roughness of 0.4 nm (Table III). However, the surface being RIE treated with pure oxygen is rougher, with a "grasslike" appearance and has a higher rms roughness of 18.2. The CF_4 treated and untreated surfaces are topographically similar in the appearance, but the level of the roughness is higher for the former. RIE with the O_2+CF_4 mixture gives rise to rms roughness of 2.5 nm in the form of ripple on the surface. The roughness values are slightly higher compared to the untreated polymer surface, but far from being high enough to provide mechanical interlocking sites.

TABLE III. Roughness values (R_a and rms) of the SU-8 surfaces obtained from AFM measurements.

Treatment	rms roughness (nm)	R_a roughness (nm)
Untreated	0.4	0.3
RIE treated with O_2	18.2	12.7
RIE treated with CF_4	2	1.6
RIE treated with O_2-rich O_2/CF_4	2.5	2

The feed gas employed plays a dominant role in the determination of the topography. In the RIE pretreatment with pure oxygen, the oxygenation of the polymer radical site causes the formation of peroxy or alkoxy radicals, thereby weakening the adjacent carbon–carbon bond and leading to chain rupture. However, atomic oxygen is very reactive species in O_2 plasma[21–23] and can react with aromatic ring to form phenols in the addition reaction without forming free radicals which could assist cleavage of the polymer backbone.[24,25] Hence, the sites of yet unsaturated (aromatic) should be more resistant to etching than the saturated sites. As a result, the grass-like surface is formed. On the other hand, etching proceeds through a saturated intermediate and fluorine species is more effective in attacking unsaturated sites than oxygen species, leading to saturated intermediates which have to undergo further reaction for etching.[24,26,27] Therefore, the introduction of a small amount of CF_4 into O_2 gradually increases the proportion of saturated bonds and equalizes the etching speed, yielding smoother surface morphology.

As no significant topographical changes (in the nm scale) on the surface RIE treated with gas mixture (O_2+CF_4) were detected by AFM measurements, the measured high adhesion strength suggests that the chemical changes at the interface enhanced the adhesion significantly.

C. Surface free energy

The RIE with O_2-rich gas mixture (O_2+CF_4) has a significant effect on the polar surface free energy γ_S^p, as reflected by the contact angle measurements. The contact angles and surface free energy on the RIE treated surface with different treatment times (15 sccm O_2

TABLE IV. Contact angles and surface free energy on the RIE treated surface with different treatment times (15 sccm O_2+5 sccm CF_4, 80 W).

RIE treatment Time (min)	Contact angle (deg) H_2O	DIM	Surface free energy (mJ/m^2) γ_S	γ_S^d	γ_S^p	Polarity (%) x^p
0	79	32	44.1	40.5	3.6	8.2
5	74	49	38.8	30.4	8.4	21.6
10	64	52	42.5	27.0	15.5	36.5
15	63	54	42.5	25.7	16.8	39.5
20	65	59	40.0	23.1	16.9	42.3

+5 sccm CF_4,80 W) are presented in Table IV. The decrease in the contact angle is indicative of the magnitude of the chemical changes taking place at the polymer surface due to the RIE treatment, which improves the surface wettability. Moreover, a strong increase in the polar surface free energy (γ_S^p), the surface polarity ($x^p = \gamma_S^p/\gamma_S$), and a decrease in the dispersion surface free energy (γ_S^d) were obtained after the RIE treatment with O_2-rich gas mixture of O_2+CF_4 for 20 min. The respective values varied from 3.6 to 16.9 mJ/m^2 for γ_S^p, from 8.2% to 42.3% for x^p, and from 40.5 to 23.1 mJ/m^2 for γ_S^d. These results indicate a highly polar polymer surface and are well correlated to the measured pull strength values.

D. XPS analysis

In order to investigate the state of chemical bonding and compositional changes of the modified polymer surface, XPS analyses were performed. The XPS wide scan spectra of the untreated SU-8 and treated SU-8 surface are shown in Fig. 8. The changes in the O to C atomic ratios are shown in Table V. These were determined from the corrected C 1*s* and O 1*s* core-level spectral peak-area ratios.[28] The treated surface with the oxygen-rich gas mixture (O_2+CF_4) has the composition of 29% O, 68% C, and 3% F, while the original polymer surface has 17% O and 83% C. This indicates strong increase in the O–to–C ratio and therefore reflects an augmented oxidation as compared with the elemental composition of the original epoxy surface. The relationship between the adhesion and the O–to–C ratio is given in Fig. 9. The higher the O–to–C ratio the stronger the adhesion. The treatment causes the breakage of some C–C or C–H bonds. The subsequent exposure of the activated surface to plasma causes oxygen to be incorporated on the polymer surface, thus leading to surface oxidation.

Further analysis of functional groups on the surface was performed using high-resolution C 1*s* spectrum from the samples. High-resolution XPS spectra in the C 1*s* region for the untreated and treated films are shown in Figs. 10(a)–10(d). The C 1*s* spectrum for the untreated SU-8 consists of two components. The one at 284.5 eV is attributed to the presence of hydrocarbons (C–C and C–H), and the other at 286.2 eV is attributed to C–O. The deconvolution of C 1*s* spectrum obtained from the surfaces treated by pure oxygen exhibits the same features as the original polymer surface in terms of the number and the types of peaks [Fig. 10(b)]. The results indicate that practically no oxidation has occurred. In this case the adhesion is weak. In the spectrum of the CF_4 treated surface [Fig. 10(c)], new peaks are located at 289.1 and 291.5 eV, which are assigned to CF and CF_2, respectively. However, these functional groups have poor adhesion to Cu or Cr. The spectrum of C 1*s* for the O_2-rich gas mixture (O_2+CF_4) treated sample shows the presence of two new oxidation bonds assigned to C=O/O–C–O at 287.3 eV and O–C=O at 288.5 eV [Fig. 10(d)]. The relative concentrations of these two oxidized carbon species are 6% and 11%, respectively. It is expected that the carbon radicals generated by the RIE treatment react with oxygen to form peroxide groups, and the peroxide groups are further modified into oxygen functional groups.

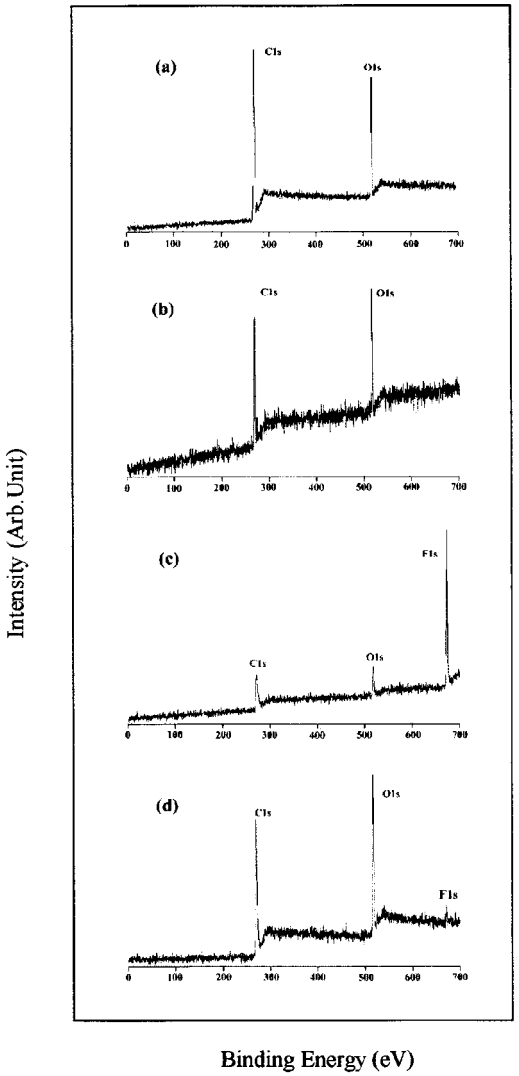

FIG. 8. XPS wide scan spectra, obtained at the photoelectron takeoff angle of 42°±2° for SU-8 (a) no treatment; (b) O_2 treatment; (c) CF_4 treatment; (d) O_2+CF_4 treatment.

TABLE V. Atomic composition of photoresist as determined by the XPS analyses (%).

Treatments	Components C	O	F	Atomic ratio O/C
Untreated	82.8	17.2		0.21
Treated with O_2	79.5	20.5		0.26
Treated with CF_4	50.2	11.9	37.9	0.24
Treated with O_2 rich O_2/CF_4	68.3	28.7	3	0.42
Treated with same amount O_2/CF_4	53.9	20.9	25.3	0.39

The C 1*s* and O 1*s* narrow spectra of the SU-8 surfaces without treatment, and those treated with the O_2, CF_4, and O_2+CF_4 are compared in Fig. 11. The peak intensities in the low-energy region shown in the C 1*s* spectra are much lower when pure CF_4 is used than when mixed gas is used. The excessive chemical modification may cause the weak bonding structure when pure CF_4 is used. In addition, the high degree of fluorination decreases the surface energy of the modified polymers resulting in poor adhesion. On the other hand, when RIE with mixed gas is used, the degree of molecular destruction is lower, and the augmented oxidation of the polymer surfaces shown in the O 1*s* spectra contributes to the increase of adhesion strength.

Chromium has high affinity to oxygen and can strongly bond to oxidized polymer surfaces.[29–34] For example, it can interact initially with the carbonyl groups to form Cr–O–C bonds or complex. The functional groups identified as C=O/O–C–O and O–C=O bonds were formed on the treated surface, as detected by XPS. Therefore, the adhesion improvement can be attributed to chemical effects, i.e., chemical bonds between chromium and oxygen.

E. Observations of fracture surfaces

The fracture surfaces of the specimens were examined with SEM to identify the failure modes and to provide qualitative assessment of the adhesion of Cu or Cr to SU-8. In most cases, the failure occurs as a complete adhesive fracture along the interface between Cr or Cu and SU-8 (Table III).

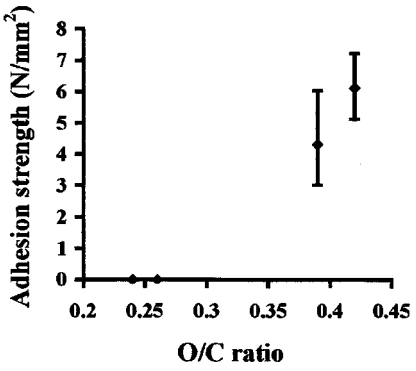

FIG. 9. Relationship between O/C ratio and average pull strength.

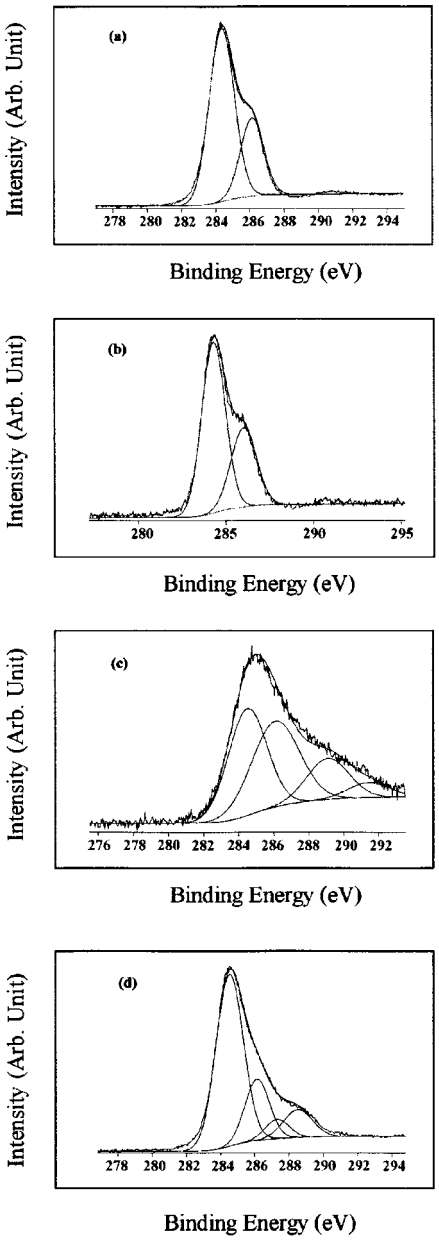

FIG. 10. C 1*s* core level spectra of SU-8 surface (not in the same scale) (a) no treatment; (b) O_2 treatment; (c) CF_4 treatment; (d) O_2+CF_4 treatment.

However, when Cr is used as the adhesion promoter and when the O_2-rich O_2+CF_4 RIE surface modification with the optimal parameters is used, cohesive failure is observed within the polymer, as confirmed by SEM (see Fig. 12). When the adhesion is increased, the locus of failure shifts further from the interface within the polymer. In fact, some-

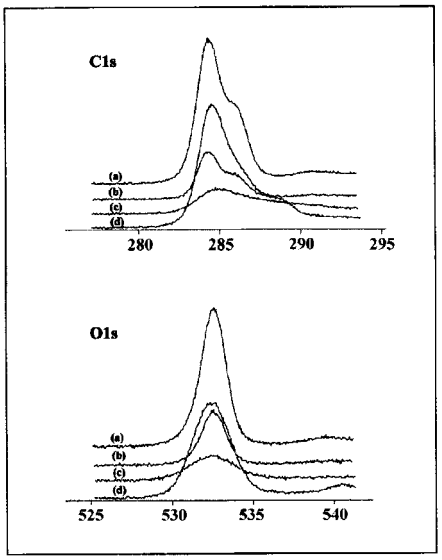

FIG. 11. Comparison of C 1*s*, O 1*s* XPS peak shape for SU-8 (in the same scale) (a) no treatment; (b) O_2 treatment; (c) CF_4 treatment; (d) O_2+CF_4 treatment.

times the failure also occurred partially inside the substrate, since glass fibers of FR4 could be observed on the epoxy side after the pull test. This suggests that the adhesion strength at the SU-8/Cr/Cu interface is much stronger than at the failed site. In some cases, fracture occurred at the WBL/bulk interface. This is because the excessive treatment of polymer results in a weak boundary layer at the surface that does not strongly adhere to the bulk.

IV. CONCLUSIONS

The adhesion of Cu or Cr/Cu to the multifunctional photoresist which was modified with chemical, plasma, and RIE treatment was investigated. The adhesion results showed that out of all the surface pretreatments used in this work, the reactive ion etching with the oxygen-rich gas mixture (O_2+CF_4) improved the adhesion significantly in the case of Cr/Cu metallization. The failure was observed to be cohesive in nature. As no significant topographical changes (in the nm scale) on the surface RIE treated with the gas mixture (O_2+CF_4) were detected by AFM measurements, the adhesion improvement is not due to the mechanical interlocking, but might be attributed to the chemical interactions at the interface. Furthermore, the XPS analyses revealed that the oxygen concentration on the surface of the polymers increased remarkably, and the functional groups were formed, which were identified as C=O/O–C–O and O–C=O bonds. The incorporation of oxygen decreased the water contact angle and strongly increased the surface polarity. The newly formed functional groups on the modified surfaces were

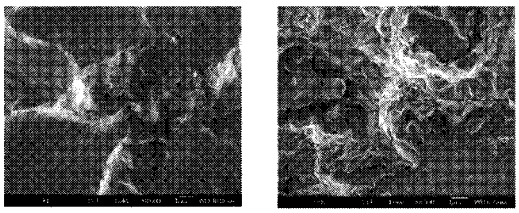

FIG. 12. SEM micrographs of typical fracture surfaces after the pull test (15 sccm O_2+5 sccm CF_4,80 W,20 min): (a) photosensitive SU-8 side; (b) backside of the test pad.

available as bonding sites for the sputter-deposited metal overlayer, and thereby good adhesion was achieved.

ACKNOWLEDGMENTS

The authors are grateful to Dr. Jouko Lahtinen and M.Sc. Mikko Hakala in the Laboratory of Physics for their helps in XPS studies. We also would like to thank Dr. Kari Lounatmaa, Dr. Sami Franssila, Dr. Victor Ovchinnicov, M.Sc. Paula Heikkilä, M.Sc. Tuuli Juvonen, and M.Sc. Antti Niskanen from the Microelectronics Center for their assistance. The academy of Finland is acknowledged for the financial support.

[1] A. Kujala, R. Tuominen, and J. K. Kivilahti, Proceedings of 49th Electronic Component Technology Conference (ECTC), 1999, USA, p. 155.
[2] T. F. Waris, R. Tuominen, and J. K. Kivilahti, Proceedings of First International IEEE Conference on Polymers and Adhesives in Microelectronics and Photonics, 2001, Potsdam, Germany, p. 218.
[3] *Metallized Plastics: Fundamentals and Applications*, edited by K. L. Mittal (Marcel Dekker, New York, 1998).
[4] D. M. Brewis, *Surface Analysis and Pretreatment of Plastics and Metal* (Applied Science, London, 1982).
[5] P. K. Wu and T.-M. Lu, Appl. Phys. Lett. **71**, 2710 (1997).
[6] H. Kupfer and G. K. Wolf, Nucl. Instrum. Methods Phys. Res. B **166–167**, 722 (2000).
[7] C. Haag and H. Suhr, Appl. Phys. A: Solids Surf. **47**, 199 (1988).
[8] J. Ge, R. Tuominen, and J. K. Kivilahti, J. Adhes. Sci. Technol. **15**, 1133 (2001).
[9] R. Heinz, E. Klusmann, H. Meyer, and R. Schulz, Surf. Coat. Technol. **116–119**, 886 (1999).
[10] P. Barnwell, J. Wood, C. Free, and D. Q. Li, Proc. SPIE **3235**, 338 (1997).
[11] T. Miyagi, Y. Iseki, K. Higuchi, Y. Shizuki, T. Hanawa, E. Takagi, M. Saito, K. Yoshihara, and M. Konno, Proceedings 46th Electronic. Component. Technology, Conference 1996, p. 149.
[12] R. L. Opila, K. Konstadinidis, and S. O'Connor, in *Polymer Surface Interfaces*, edited by K. L. Mittal and K.-W. Lee (Utrecht, Netherlands, 1997), p. 179.
[13] D. K. Owens and R. C. Wendt, J. Appl. Polym. Sci. **13**, 1741 (1969).
[14] *CRC Handbook of Chemistry and Physics*, edited by C. Weast (CRC, Boca Raton, FL, 1982).
[15] P. S. Ho, J. W. Bartha, G. W. Rubloff, F. K. LeGoues, and B. D. Silverman, J. Vac. Sci. Technol. A **3**, 739 (1985).
[16] P. O. Hahn, G. W. Rubloff, J. W. Bartha, F. K. LeGoues, R. Tromp, and P. S. Ho, in *Proceedings on Electronics Packaging and Material Science*, edited by E. Geiss, K. Tu, and D. R. Uhlmann (Materials Research Society, Pittsburgh, 1985), p. 251.
[17] M. Davie and K. F. Jensen, J. Vac. Sci. Technol. A **8**, 1648 (1990).
[18] C. J. Mogab, A. C. Adams, and D. L. Flamm, J. Appl. Phys. **49**, 3796 (1978).
[19] R. W. Burger and L. J. Gerenser, in *Metallized Plastics 3: Fundamental and Applied Aspects*, edited by K. L. Mittal (Plenum, New York, 1992). p. 179.

[20] J. Friedrich, W. E. S. Unger, A. Lippice, T. Gross, P. Rohrer, W. Saur, J. Erdmann, and H.-V. Gorsler, J. Adhes. Sci. Technol. **9**, 575 (1995).
[21] A. G. Shard and J. P. S. Badyal, J. Phys. Chem. **95**, 9436 (1991).
[22] O. Joubert, J. Pelletier, and Y. Arnal, J. Appl. Phys. **65**, 5096 (1989).
[23] *Techniques and Application of Plasma Chemistry*, edited by J. R. Hollahan and A. T. Bell (Wiley, New York, 1974), Chap. 1.
[24] D. F. Egitto, V. Vukanovic, and G. N. Taylor, in *Plasma, Deposition, Treatment, Etching of Polymers*, edited by R. d'Agostino (Academic, San Diego, 1990), Chap. 5.
[25] S. J. Moss, J. Inst. Energy **17**, 205 (1987).
[26] S. R. Cain, F. D. Egitto, and F. Emmi, J. Vac. Sci. Technol. A **5**, 1578 (1987).
[27] D. F. Egitto, V. Vukanovic, F. Emmi, and R. S. Horwath, J. Vac. Sci. Technol. B **3**, 893 (1985).
[28] J. F. Moulder, W. F. Stickle, P. E. Sobol, and K. D. Bomben, *Handbook of X-Ray Photoelectron Spectroscopy*, edited by J. Chastain (Perkin-Elmer, Eden Prairie, MN, 1990).
[29] J. M. Burkstrand, J. Appl. Phys. **52**, 4795 (1981).
[30] J. L. Jordan, C. A. Kovac, J. F. Morar, and R. A. Pollak, Phys. Rev. B **36**, 1369 (1987).
[31] J. F. Friedrich, W. E. S. Unger, A. Lippitz, I. Koprinarov, G. Kuhn, St. Weidner, and L. Vogel, Surf. Coat. Technol. **116–119**, 772 (1999).
[32] W. E. S. Unger, A. Lippitz, Th. Gross, J. F. Friedrich, Ch. Wöll, and L. Nick, Langmuir **15**, 1161 (1999).
[33] N. J. Chou, D. W. Dong, J. Kim, and A. C. Lin, J. Electrochem. Soc. **131**, 2335 (1984).
[34] Y. Nakamura, Y. Suzuki, and Y. Watanable, Thin Solid Films **290–291**, 367 (1996).